

# Corrosion protection in saline environment of a carbon steel coated (aluminum & three-layer painting system) by EATS

Protección contra corrosión en ambiente salino de aceros al carbono recubierto con aluminio-pintura por EATS

Diego Pérez-Muñoz<sup>1\*</sup>, José Luddey Marulanda-Arévalo<sup>1</sup>, Carlos Mauricio Moreno-Tellez<sup>2</sup>

<sup>1</sup>Facultad de Ingeniería Mecánica, Universidad Tecnológica de Pereira. Carrera 27 #10-02. A.A. 97. Pereira, Colombia

<sup>2</sup>Facultad de Ingeniería, Universidad Pedagógica y Tecnológica de Colombia. Avenida Central del Norte #39-115. A.A. 1094. Tunja, Colombia

## ARTICLE INFO:

Received: September 25, 2017

Accepted: September 04, 2018

## AVAILABLE ONLINE:

October 16, 2018

## KEYWORDS:

Aluminum, Corrosion, EATS, Paint, Saline environment

Aluminio, Corrosión, EATS, Pintura, Ambiente salino

**ABSTRACT:** This paper presents a comparative study on corrosion protection of low-carbon steel coated with two different painting systems. The first set of samples was coated with an aluminum layer of primer deposited by Electric Arc Thermal Spray (EATS), after which two additional layers of paint were applied, thereby creating an aluminum-painting system; while the second set of samples was coated with the traditional three-layer painting system (zinc-rich layer of primer). Afterwards, all the samples were exposed to the salt spray chamber. The samples were monitored to record their reactions in the corrosive saline environment. Scanning Electron Microscopy (SEM), adhesion and electrochemical corrosion tests were performed to characterize the coatings and report changes in their properties (adhesion, topography and homogeneity), which are related to exposure time. The three-layer painting system barely complied with manufacturer claims on protection time under corrosive conditions; on the other hand, the aluminum-painting system yielded better results by prolonging protection time.

**RESUMEN:** Este artículo presenta un estudio comparativo de protección contra la corrosión de aceros de bajo carbono recubiertos con dos sistemas diferentes de pintura. El primer grupo de muestras fue recubierto con una capa de aluminio depositada por Rociado Térmico por Arco Eléctrico (EATS por sus siglas en inglés), subsecuentemente dos capas adicionales de pintura fueron aplicadas, creando así un sistema aluminio/pintura. Mientras que, un sistema tradicional de tres capas de pintura (primera capa de pintura rica en zinc) fue depositado en el segundo grupo de muestras. Finalmente, todas las muestras fueron expuestas en la cámara de niebla salina. Las muestras fueron monitoreadas para obtener su comportamiento en el corrosivo ambiente salino. Microscopía Electrónica de Barrido (SEM por sus siglas en inglés), ensayos de adhesión y corrosión electroquímica fueron realizadas para caracterizar los recubrimientos y reportar los cambios en sus propiedades (adhesión, topografía y homogeneidad), las cuales están relacionadas con el tiempo de exposición. El sistema de tres capas escasamente cumplió con la garantía dada por su fabricante en lo referente al tiempo de protección bajo condiciones corrosivas; por otro lado, el sistema de aluminio/pintura entregó mejores resultados al prolongar el tiempo de protección.

## 1. Introduction

Most of productive installations within the manufacturing sector are made of metal; their functionality and stability are required for prolonged use during many years.

The deterioration of metal structures due to atmospheric corrosion is a recurring and severe problem leading to the loss of thousand millions of dollars every year [1-3]. During years, coatings with sacrificial metals, specifically zinc and aluminum, have been considered the best protection methods against atmospheric corrosion for steel structures, because those metals retard deterioration through time and prolong functionality. Corrosion rate depends on physicochemical properties

\* Corresponding author: Diego Pérez-Muñoz

E-mail: dperez@utp.edu.co

ISSN 0120-6230

e-ISSN 2422-2844



of material, corrosive atmosphere, and the emergence of volatile elements such as oxides, hydroxides, sulfate, carbonates or silicates [4, 5].

Zinc-rich painting technologies have been used through the years for protection in aggressive environments, like special industrial environments and sailing, among others. However, these systems require considerably thick coating in order to allow electric current flow. One of the coating systems used in this study has a zinc-rich layer of primer, an epoxy paint middle layer and a polyaspartic finishing layer.

In the initial stage of the oxidation process on steels in saline environments, the electric contact of the sacrificial anode (zinc) with the metallic substrate provides cathodic protection, which is formed from corrosion byproducts such as zinc oxides and/or hydroxides. A significant humidification of zinc particles takes place due to the coating porosity and a ratio greater than one between pigment volume concentration (PVC) and critical pigment volume concentration (CPVC). Such a ratio allows the access of water electrolyte and sacrifice task of zinc particles. Additionally, when using high content of zinc pigments (well above CPVC), the mechanical properties and homogeneity of the dry coating may deteriorate and a significant fraction of the zinc particles zinc does not participate in the sacrifice task [6–11].

On the other hand, aluminum has demonstrated good behavior against saline environments in several works [12–16], due to its great capacity to generate oxides with good mechanical and chemical properties, which do not detach easily, preventing the contact between the substrate and the environment.

Thermal spray is a metallurgic process to coat the substrate with metal layers made of a material, which can be different from the material base. The final combination is expected to yield better physical, mechanical and chemical properties, as well as cheaper maintenance costs in comparison to the usage of uncoated material. The development of new alloys and applications has contributed to the progress of thermal spray, and the advantages of this technique for parts manufacturing and maintenance have gained acceptance within the industry. Electric arc thermal spray uses a voltaic arc for heating and melting two consumable electrodes or wires electrically charged (one wire is positive “anode”, and the other negative “cathode”). An atomizing gas, usually compressed air, blows the molten metal onto the substrate. The coatings are deposited when splats of melted wire collide against the substrate, each layer solidifies and adheres almost immediately [the count is in the order of millions of particles per  $\text{cm}^2/\text{s}$ ] [11, 14].

Coating properties are related to both, their microstructure and the interface between substrate and coating layer. The shape of the deposited particles depends on their impact energy; temperature and speed of particles inside the jet flame should be also taken into account. Thermal spray process by electric arc can be used to deposit coatings of greater hardness and/or better resistance to atmosphere corrosion. This technique has not only reasonable costs but also high deposition rate; hence, these coatings are a good option to prolong the useful life of large areas on steel infrastructures like bridges [11].

The aim of this work is to perform a comparative study of the corrosion protection of low steel carbon coated with an aluminum alloy system by means of electric arc thermal spray. The morphological and corrosion behavior was studied, with a particular interest in the corrosion behavior under saline environment.

## 2. Experimental Procedure

### 2.1 Samples preparation

Twenty low-carbon-steel samples with dimensions 10 cm x 20 cm x 0.5 cm, were sandblasted during 5 minutes to obtain a roughness texture with  $R_a 5.62 \mu\text{m} \pm 0.11$ , and thereby ensuring good adherence of coatings and paints, due to the continuity between their cross-section borders [3]. Low-carbon-steel specimens with dimensions of 10 x 20 x 0.5 cm, were sandblasted for 5 min using spherical frit with hardness between up 51 HRC, with a pressure of 115 psi. Then, ten samples were coated with the traditional three-layer painting system (zinc-rich layer of primer, an epoxy paint middle layer and a polyaspartic finish layer). The remaining samples were coated using aluminum as the primer layer which was deposited by electric arc thermal spray under air pressure of 55 psi and deposition distance of 20 – 30 cm using an aluminum wire (99.5% purity) with 2 mm of diameter. The deposition rate was of  $2.7 \text{ kg/m}^2$  applying a current of 100 A.

Once the two coating systems were applied, samples were subjected to corrosion environment in a mist saline chamber abiding by ASTM B117, which pretended real saline conditions (water with 5% NaCl at 35° C), controlled and supervised getting record every single changes on the samples. Photographed inspections were done each 48 hours during first 1448 hours of exposure; afterwards, inspections took place every 168 hours, total exposure time was 2256 hours.

## 2.2 Characterization of the coatings

The characterization was carried out in three stages; before, after 1448 hours, and finally after 2256 hours of exposure. Figure 1 depicts two samples with each protective system, before exposure to saline environment. The results from characterization were the basis to analyze adherence variation, topographic changes and degradation of protective systems due to corrosion. Firstly, pull-off tests in compliance with ASTM D4541 standard were carried out to assess adherence of paints and thermal spray [15–19]; the tensile stress was applied by a manual hydraulic pump with pressure control which indicated the detachment pressure for every sample. The coatings were carried out by scanning electron microscopy (SEM) using a Phenom ProX desktop microscope equipped with energy dispersive X-ray (EDX) spectroscopy (Bruker EDS Analyzer). EDS analysis facilities to analyze qualitative and quantitative values of the two coating systems studied herein; its acceleration voltage was 15kV, an EDX detector Bruker and high vacuum mode. Protective properties of both systems were also compared based on the corrosion rates revealed after electrochemical tests. In addition, electrochemical test was assessed by means of potentiodynamic polarization measurements; the electrode used as reference was Ag/AgCl, scanning rate of  $\pm 1 \text{ mV/s}$ , a counter electrode of platinum, the environment was brine with 3.5% of salt (relation volume/weight); all of them are part of electrochemical cell of three electrodes.

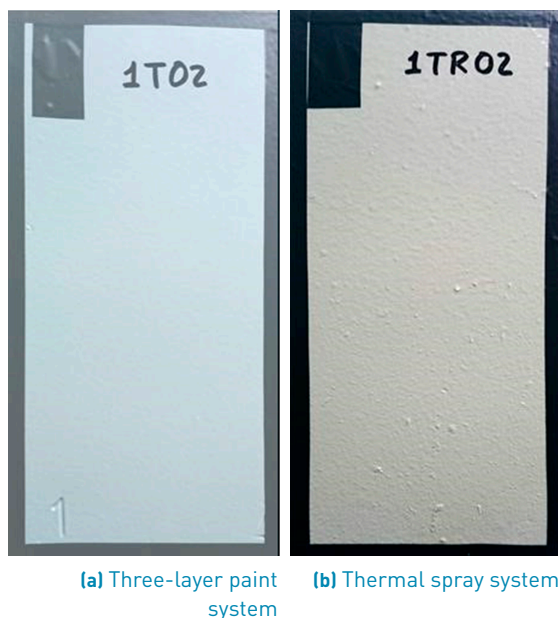


**Figure 1** Samples with three-layer system and thermal spray plus paint system before exposure to saline environment

## 3. Results and analysis

Neither of the two systems exhibited deterioration signs when the first stage of characterization took place (1448 hours), this behaviour is in accordance with the claims of manufacturer for the case of the three-layer painting system. To accelerate the corrosion process, ASTM B117 standard suggests to scratch the surface of samples.

The performance of both protective systems after 1920 hours of oxidation can be seen in Figure 2. Figure 2a corresponding to the three-layer paint system shows substrate oxidation due to formation of iron oxides, which in turn interfere with coating adherence and accelerate the detriment of the paint properties. In contrast, the thermal spray system does not present iron oxides, because aluminum layer created an alumina layer of white colour that protects the substrate from oxidation [18–20] without affecting paint adherence (Figure 2b). Adherence tests confirmed the above.

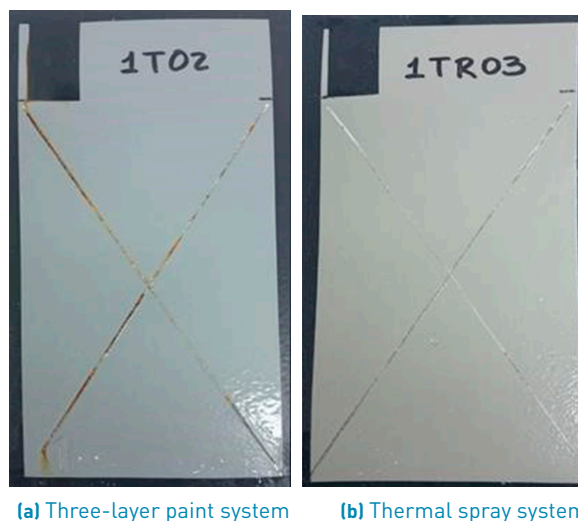
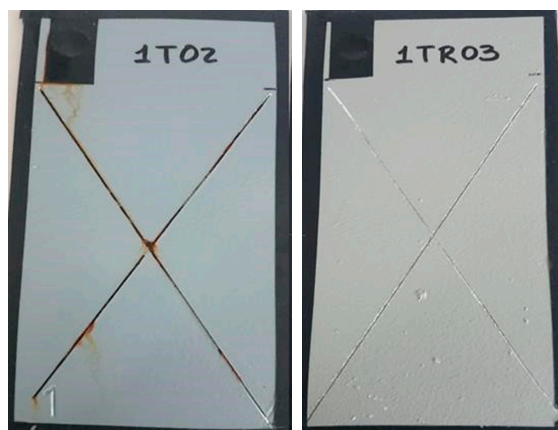


**Figure 2** Specimens with three-layer system and thermal spray system oxidized after 1920 hours

Behavior trends of the two protective systems remained the same after 2256 hours of oxidation (Figure 3). As far as the three-layer system is concerned, iron oxides become more noticeable not only all along of the scratches, but also in their intersection. There are also several points of painting detachment due to the oxide layer (Figure 3a). Whereas small alumina blisters appeared on the scratches of thermal spray system improving oxidation resistance (Figure 3b).

Tables 1 and 2 detailed the behavior of pressure and adherence during Pull-Off test for both protective systems. The tables also report higher pressures for the



(a) Three-layer paint system (b) Thermal spray system

**Figure 3** Specimens with three-layer system and thermal spray system oxidized after 2256 hours

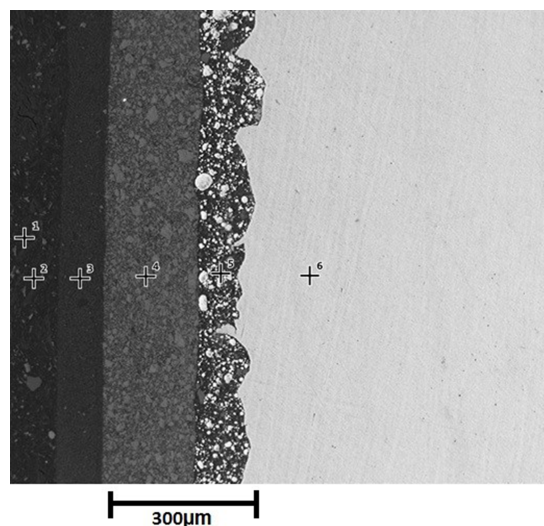


**Figure 4** Cross section of Three-layer paint system sample before oxidation

thermal spray system to remove the dollies. With the first dollies removal after 1440 hours, thermal spray system was only affected by a 39,62% of coating detachment that only included the external layer of polyaspartic. While three-layer paint system was affected by a 48,27% of coating detachment that included the external layer of Polyaspartic and epoxy barrier. Despite percentages of adherence decreased during longer periods of exposure for both systems, the adherence loss is less accelerated in the case of three-layer paint system.

**Table 1** Pull-off test of three-layer paint system

Exposure Time (Hours)	Pressure (psi)	Adherence (%)
0	618	51.73
1440	208.5	37.97
2256	201.3	27.86

**Table 2** Pull-off test of thermal spray system

Exposure Time (Hours)	Pressure (psi)	Adherence (%)
0	723	69,51
1440	354.75	60.38
2256	207.75	55.25

### 3.1 Morphological and chemical observations

Figure 4 shows a cross section of three-layer paint system before exposure to saline environment. Points 1 and 2 correspond to the resin, point 3 represents the Polyaspartic finish layer, point 4 depicts the epoxy barrier

and finally the zinc rich primer and the substrate are indicated by point 5 and 6 respectively. The morphology of three-layer paint system shows low porosity (4.5%), reported by microscopy techniques, no micro cracks and contact between zinc particles and substrate (allowing cathodic protection of substrate). Figure 4 attests to the continuity of the paint-substrate interphase, which suggests good adherence of painting to substrate thanks to rugosity on the substrate provided by sandblasting [20].

The complement of morphological and chemical characterization was carried out with EDS analysis, showing the chemical composition reports on the cross section of sample (Table 3).

**Table 3** EDS analysis corresponding to three-layer paint system before oxidation

Point	Element	Quantity (%)
3 (polyaspartic)	Titanium	60
	Oxygen	10.3
	Carbon	29.7
4 (epoxy barrier)	Antimony	42.9
	Barium	21.2
	Oxygen	26.2
	Carbon	9.7
5 (rich zinc primer)	Zinc	90.1
	Oxygen	4.0
	Carbon	5.9
6 (substrate)	Iron	92
	Oxygen	5.8
	Carbon	2.2



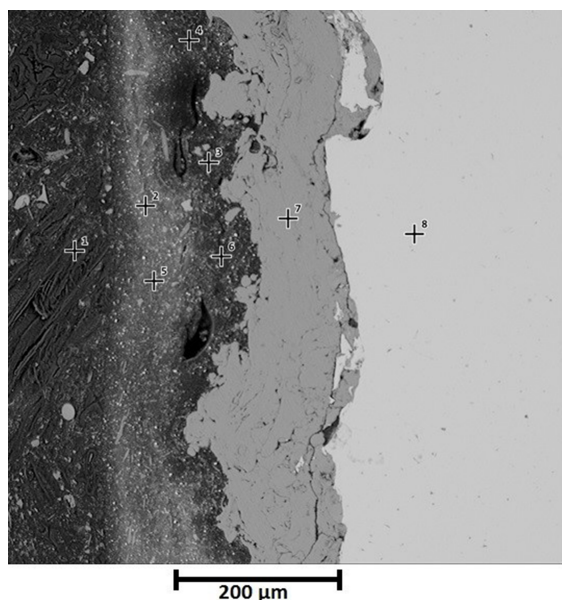


**Figure 5** Cross section of thermal spray and paint system before exposure

Cross section of thermal spray system before exposure to saline environment can be seen in Figure 5. Points 1 depicts the resin, polyaspartic finish layer is indicated by points 2 and 5, points 3, 4 and 6 represent epoxy barrier and finally points 7 and 8 correspond to aluminum layer and substrate respectively. For thermal spray system, good adherence was not only verified in substrate-coating interphase but also in coating-paint interphase. Since the aluminum deposited replicated the roughness obtained after sandblasting. It is important to clarify that the spaces observed on the Figure 5 are characteristic of paint, not of the interphase paint - aluminum layer. For that reason, the appreciation of good adherence is in accordance with Pull Off tests.

EDS analysis corresponding to thermal spray system before oxidation, delivered the following chemical composition showed in the Table 4:

Aiming to keep track of changes in adherence and chemical composition of samples, SEM and EDS analysis were performed after 2256 hours of exposure. In relation to the three-layer paint system, SEM cross section view (Figure 6) and Table 5 compare the topography of every zone and their chemical composition.

In SEM cross section view of sample with thermal spray system (Figure 7) after 2256 hours of oxidation, only porosities in the epoxy layer can be seen rather than the clearances reported for the epoxy barrier of three-layer paint system. Besides, in this figure, the substrate zone looks planer than other figures, because the sandblasting

**Table 4** EDS analysis corresponding to thermal spray system before oxidation

Point	Element	Quantity (%)
2 and 5 (polyaspartic)	Titanium	47.2
	Oxygen	21.6
	Carbon	31.2
3, 4 and 6 (epoxy barrier)	Antimony	31.6
	Barium	7.5
	Oxygen	39.1
	Carbon	21.8
7 (aluminum layer)	Aluminum	72.8
	Oxygen	18
	Carbon	9.2
6 (substrate)	Iron	91.8
	Oxygen	6
	Carbon	2.2

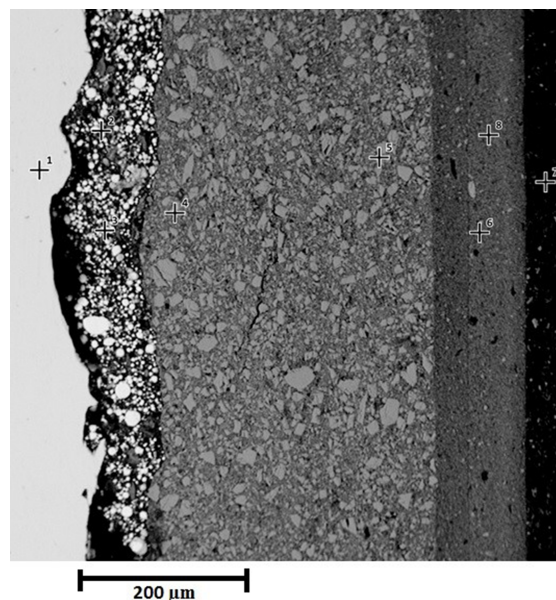


**Figure 6** Cross section of three-layer paint system after 2256 hours of oxidation

process was carried out by human workers; they must guarantee 90° between sand yet and the sample surface, but this aim is not always successful. Characterized zones and their corresponding chemical composition (%) are namely the following Table 6.

**Electrochemical Corrosion Tests**

Linear Polarization Resistance (LPR) was used to relate current density and corrosion potentials, the resulting slopes are shown in Figure 8. LPR was estimated after 1448 and 2256 hours of oxidation; electrochemical tests was unfeasible for samples before oxidation due to electrochemical circuit isolation [21-23]. During oxidation from zinc to divalent zinc, the release of electrons flowing

**Table 5** EDS analysis corresponding to three-layer paint system after 2256 hour of exposure

Point	Element	Quantity (%)
1 (substrate)	Iron	75
	Oxygen	20.5
	Carbon	4.5
2 and 3 (rich zinc primer)	Zinc	60
	Carbon	8.4
4 and 5 (epoxy barrier)	Antimony	26.4
	Barium	4.4
	Oxygen	56.4
	Carbon	12.8
2 and 3 (polyaspartic)	Titanium	28.2
	Oxygen	46.1
	Carbon	25.7

**Table 6** EDS analysis corresponding to thermal spray system after 2256 hour of exposure

Point	Element	Quantity (%)
1 (substrate)	Iron	93.2
	Oxygen	3.8
	Carbon	3.0
2 and 4 (aluminum layer)	Aluminium	93
	Carbon	1.1
3, 5, 7 and 8 (epoxy barrier)	Antimony	26.1
	Barium	4.6
	Oxygen	61.6
	Carbon	7.7
6 (polyaspartic)	Titanium	41.5
	Oxygen	36.1
	Carbon	22.4

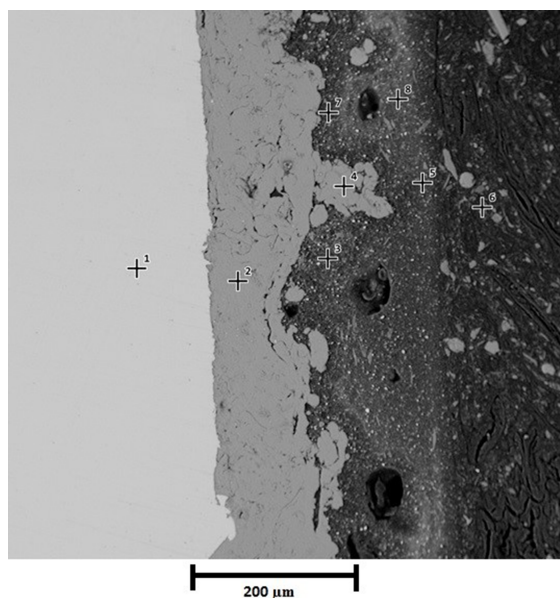


**Figure 7** Cross section of thermal spray system after 2256 hours of oxidation

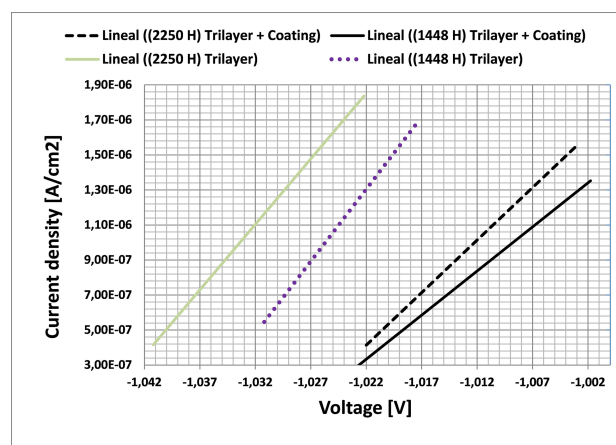


**Figure 8** Linear polarization lines of resistance and elongation for three-layer systems with thermal spraying

through the coating film contributed with the cathodic protection of steel substrate against blistering. This protection starts to take place when corrosion potentials of the coating systems are less than that of silver from electrochemical device (-0.80 V). Corrosion potentials reported on Figure 8 averaged -1.0 V for both coating systems and slightly decreased with longer exposure times. The painting system presented steeper slopes than thermal spray system. According to slopes of Figure 8, current density is directly proportional to corrosion rates; thus, less steep slopes imply better protection [23–26].

As a second step in electrochemical corrosion tests, TAFEL curves (Figure 9) illustrate the relation between current density and corrosion potential plus reference

electrode (ER). In this figure, it is demonstrated that the corrosion potentials for three-layer painting system are close to each other, being negative both (between -1.0 V y -1.2 V); moreover, they are lower than substrate corrosion potential, validating that idea that there are cathodic protection of zinc pigments, while thermal spray system curves presents high separation (between -0.7 V and -0.95 V), which indicates that to 1440 hours there was a partial substrate cathodic protection, but when time increased (2250 hours), the system reached a total cathodic protection, because it had 150 mV more negative in comparison with the substrate (steel) corrosion potential for reference electrode of device used (-0.80 V), for this reason, the system has enough electromotive force to the cathodic protection of substrate; the above due to the aluminum and/or zinc active dissolution. Nevertheless, the separation of substrate curves is higher in comparison with the other ones studied, reporting highest corrosion rates. On the other hand, the corrosion rate is very low for

both systems (Three-layer Painting System and Thermal Spray System), generating a protection of zinc and aluminum pigments respectively; although there is a little consumption increase of current density in 2250 hours, for both systems, fact that raises zinc and aluminum consumption, forming oxides: The above phenomena are corroborated on the SEM images, leading to lose of paint adherence and an increment of rate corrosion [27–33].

Based on the literature, the corrosion current for low carbon steels is in average  $1.4 \times 10^{-4} A/cm^2$  [34, 35], and the thermal spray system reported in average  $1.2 \times 10^{-5}$ , while three-layer painting system reported  $1.8 \times 10^{-5} A/cm^2$ ; this information is observable on Figure 9.

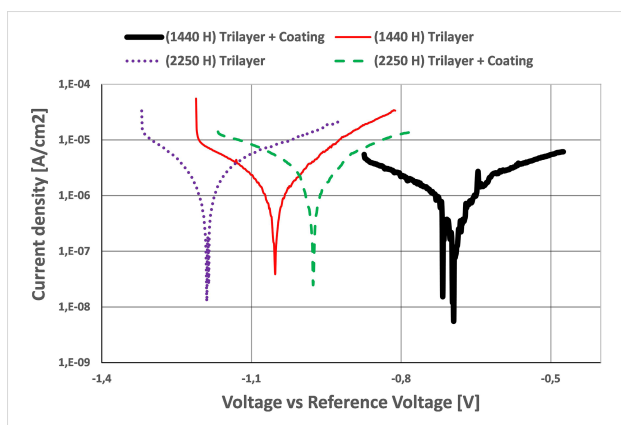


**Figure 9** TAFEL curves for three-layer system and thermal spray system

## 4. Conclusions

Aluminum layer deposited by electric arc thermal spray technique, provides a better protection against corrosion in saline environments in comparison to three-layer painting system, even after scratching samples (1440 hours) with the purpose to worsen corrosion conditions; owing to the fact that aluminum has better galvanic protection properties than zinc, preventing that iron oxides are formed on substrate.

Pull Off tests indicate that adherence and pressure for both protective systems were similar before the samples got in to mist saline chamber, these values changed when exposition time increased. The values decreased considerably, being more notorious the decreasing in three-layer paint system samples, because when they were oxidized, layers of paint lose adherence, causing separation between them and substrate; doing easier the contact of saline environment to substrate.

The corrosion rate in the three-layer painting system samples is much greater than the thermal spray samples, increasing that speed with the exposition time in saline environment. That information obtained from Linear Polarization Resistance LPR and curves TAFEL, corroborates the concept of protections against corrosion in saline environments provided by aluminum.

The minimum time of protection in mist saline guaranteed by manufacturer for Three-layer paint system (1440 hours) was achieved successfully, although some little points appeared oxidized on the porous of paint after 1558 hours of exposition.

## 5. Acknowledgements

Financial support from COLCIENCIAS Colombia by the scholarship JOVEN INVESTIGADOR (M101PR03F09).

Laboratories and devices provided by Centro de Ensayos y Consultoría en Ensayos No Destructivos CECEND, Universidad Tecnológica de Pereira.

Mechanical and chemical characterization of samples by Servicio Nacional de Aprendizaje SENA.

## References

- [1] H. Y. Li, J. Y. Duan, and D. D. Wei, "Comparison on corrosion behaviour of arc sprayed and zinc-rich coatings," *Surface and Coatings Technology*, vol. 235, pp. 259–266, Nov. 2013.
- [2] H. S. Lee, J. K. Singh, and J. H. Park, "Pore blocking characteristics of corrosion products formed on aluminum coating produced by arc thermal metal spray process in 3.5 wt.% nacl solution," *Construction and Building Materials*, vol. 113, pp. 905–916, Jun. 2016.
- [3] J. L. Marulanda, J. L. Tristanco, and H. A. González, "La tecnología de recuperación y protección contra el desgaste está en el rociado térmico," *Revista Prospectiva*, vol. 12, no. 1, pp. 70–78, Jan. 2014.
- [4] J. L. Marulanda and J. L. Tristanco, *Rociado térmico*, 1st ed. Pereira, Colombia: Universidad Tecnológica de Pereira, 2015.
- [5] J. E. Montoya, F. Vargas, and J. A. Calderón, "evaluación de la capacidad protectora de recubrimientos Ni-SiC y Ni-Co-W depositados por proyección térmica," *Dyna*, vol. 76, no. 160, pp. 195–206, 2009.
- [6] E. Armelin and et al., "Corrosion protection with polyaniline and polypyrrole as anticorrosive additives for epoxy paint," *Corrosion Science*, vol. 50, no. 3, pp. 721–728, Mar. 2008.
- [7] K. Schaefer and A. Miszczyk, "Improvement of electrochemical action of zinc-rich paints by addition of nanoparticulate zinc," *Corrosion Science*, vol. 66, pp. 380–391, Jan. 2013.
- [8] E. Akbarinezhad, M. Ebrahimi, F. Sharif, and A. Ghanbarzadeh, "Evaluating protection performance of zinc rich epoxy paints modified with polyaniline and polyaniline-clay nanocomposite," *Progress in Organic Coatings*, vol. 77, no. 8, pp. 1299–1308, Aug. 2014.
- [9] A. A. Guzmán and L. M. Ocampo, "Evaluación de la resistencia a la corrosión del sistema primer epóxico rico en zinc/acabado polisiloxano por medio de espectroscopia de impedancia electroquímica," *Dyna*, vol. 78, no. 167, pp. 87–95, 2011.
- [10] H. F. Rojas, J. J. Olaya, and C. A. Molina, "Caracterización morfológica de los recubrimientos 140mxc-530as y 140mxc-560as

- usando la técnica de proyección térmica por arco eléctrico," *Ingeniería, Investigación y Tecnología*, vol. 17, no. 1, pp. 1–13, Jan. 2016.
- [11] J. L. Marulanda, J. L. Trisancho, and L. A. Cañas, "Protección contra la corrosión en sales fundidas de un acero hot rolled, en el rango de temperaturas de 400 °C–600 °C, recubierto por rociado térmico con acero inoxidable 312," *Dyna*, vol. 76, no. 160, pp. 229–235, 2009.
- [12] H. A. M. Muhamad, N. H. Saad, S. K. Abas, N. R. N. Roselina, and M. S. Noriyati, "Performance and microstructure analysis of 99.5coating by thermal arc spray technique," *Procedia Engineering*, vol. 68, pp. 558–565, 2013.
- [13] R. M. H. Pombo, R. S. C. Paredes, S. H. Wido, and A. Calixto, "Comparison of aluminum coatings deposited by flame spray and by electric arc spray," *Surface and Coatings Technology*, vol. 202, no. 1, pp. 172–179, Nov. 2007.
- [14] M. K. Hedges, A. P. Newbery, and P. S. Grant, "Characterisation of electric arc spray formed ni superalloy in718," *Materials Science and Engineering: A*, vol. 326, no. 1, pp. 79–91, Mar. 2002.
- [15] J. E. Muñoz and J. J. Coronado, "Análisis mecánico y tribológico de los recubrimientos Fe-Cr-Ni-C y Ni-Al-Mo," *Dyna*, vol. 74, no. 153, pp. 111–118, 2007.
- [16] A. P. Newbery and P. S. Grant, "Oxidation during electric arc spray forming of steel," *Journal of Materials Processing Technology*, vol. 178, no. 1-3, pp. 259–269, Sep. 2006.
- [17] W. L. Hsu, H. Murakami, J. W. Yeh, A. C. Yeh, and K. Shimoda, "On the study of thermal-sprayed Ni<sub>0.2</sub>Co<sub>0.6</sub>Fe<sub>0.2</sub>CrSi<sub>0.2</sub>AlTi<sub>0.2</sub> HEA overlay coating," *Surface and Coatings Technology*, vol. 316, pp. 71–74, Apr. 2017.
- [18] F. Ahnia and B. Demri, "Evaluation of aluminum coatings in simulated marine environment," *Surface and Coatings Technology*, vol. 220, pp. 232–236, Apr. 2013.
- [19] A. Perez and *et al.*, "Influence of metallurgical states on the corrosion behaviour of Al-Zn PVD coatings in saline solution," *Corrosion Science*, vol. 74, pp. 240–249, Sep. 2013.
- [20] M. Barletta, A. Gisario, M. Puopolo, and S. Vesco, "Scratch, wear and corrosion resistant organic inorganic hybrid materials for metals protection and barrier," *Materials & Design*, vol. 69, pp. 130–140, Mar. 2015.
- [21] H. Shi, F. Liu, and E. H. Han, "The corrosion behavior of zinc-rich paints on steel: Influence of simulated salts deposition in an offshore atmosphere at the steel/paint interface," *Surface and Coatings Technology*, vol. 205, no. 19, pp. 4532–4539, Jun. 2011.
- [22] L. Veleva, J. Chin, and B. del amo, "Corrosion electrochemical behavior of epoxy anticorrosive paints based on zinc molybdenum phosphate and zinc oxide," *Progress in Organic Coatings*, vol. 36, no. 4, pp. 211–216, Sep. 1999.
- [23] Q. Jiang and *et al.*, "Electrochemical corrosion behavior of arc sprayed Al-Zn-Si-RE coatings on mild steel in 3.5% nacl solution," *Transactions of Nonferrous Metals Society of China*, vol. 24, no. 8, pp. 2713–2722, Aug. 2014.
- [24] Y. F. Yan and *et al.*, "Hot corrosion behaviour and its mechanism of a new alumina-forming austenitic stainless steel in molten sodium sulphate," *Corrosion Science*, vol. 77, pp. 202–209, Dec. 2013.
- [25] Q. X. Fan, S. M. Jiang, H. J. Yu, J. Gong, and C. Sun, "Microstructure and hot corrosion behaviors of two co modified aluminide coatings on a ni-based superalloy at 700 °C," *Applied Surface Science*, vol. 311, pp. 214–223, Aug. 2014.
- [26] R. Li, Z. Zhou, D. He, L. Zhao, and X. Song, "Microstructure and high-temperature oxidation behavior of wire-arc sprayed fe-based coatings," *Surface and Coatings Technology*, vol. 251, pp. 186–190, Jul. 2014.
- [27] M. Hafiz, N. Hayati, S. Kiyai, and N. Mohd, "Thermal arc spray overview," in *IOP Conf. Series: Materials Science and Engineering*, Bandung, Indonesia, 2013, pp. 1–10.
- [28] L. Baiamonte and *et al.*, "Thermal sprayed coatings for hot corrosion protection of exhaust valves in naval diesel engines," *Surface and Coatings Technology*, vol. 295, pp. 78–87, Jun. 2016.
- [29] G. A. Awadi, S. Abdel, and E. S. Elshazly, "Hot corrosion behavior of ni based inconel 617 and inconel 738 superalloys," *Applied Surface Science*, vol. 378, pp. 224–230, Aug. 2016.
- [30] B. Salehnasab, E. Poursaeidi, S. A. Mortazavi, and G. H. Farokhian, "Hot corrosion failure in the first stage nozzle of a gas turbine engine," *Engineering Failure Analysis*, vol. 60, pp. 316–325, Feb. 2016.
- [31] H. He, Z. Liu, W. Wang, and C. Zhou, "Microstructure and hot corrosion behavior of Co-Si modified aluminide coating on nickel based superalloys," *Corrosion Science*, vol. 100, pp. 466–473, Nov. 2015.
- [32] T. Gheno, M. Zahiri, A. H. Heuer, and B. Gleeson, "Reaction morphologies developed by nickel aluminides in type ii hot corrosion conditions: The effect of chromium," *Corrosion Science*, vol. 101, pp. 32–46, Dec. 2015.
- [33] Z. Xu and *et al.*, "Isothermal oxidation and hot corrosion behaviors of diffusion aluminide coatings deposited by chemical vapor deposition," *Journal of Alloys and Compounds*, vol. 637, pp. 343–349, Jul. 2015.
- [34] Y. Liu, B. Zhang, Y. Zhang, L. Ma, and P. Yang, "Electrochemical polarization study on crude oil pipeline corrosion by the produced water with high salinity," *Engineering Failure Analysis*, vol. 60, pp. 307–315, Feb. 2016.
- [35] Y. Zou, J. Wang, and Y. Y. Zheng, "Electrochemical techniques for determining corrosion rate of rusted steel in seawater," *Corrosion Science*, vol. 53, no. 1, pp. 208–216, Jan. 2011.